Before The San Juan Basin: An Overview Of The Upper Cretaceous Western Interior Seaway

Bruce S. Hart

2025, pp. 123-136. https://doi.org/10.56577/FFC-75.123

in:

Geology of the Eastern San Juan Basin - Fall Field Conference 2025, Hobbs, Kevin M.; Mathis, Allyson; Van Der Werff, Brittney;, New Mexico Geological Society 75 th Annual Fall Field Conference Guidebook, 227 p. https://doi.org/10.56577/FFC-75

This page is intentionally left blank to maintain order of facing pages.

New Mexico Geological Society Guidebook, 75th Fall Field Conference, 2025, p. 123–136, https://doi.org/10.56577/FFC-75.123

BEFORE THE SAN JUAN BASIN: AN OVERVIEW OF THE UPPER CRETACEOUS WESTERN INTERIOR SEAWAY

BRUCE S. HART[1]

[1]Department of Earth Sciences, Western University, London, ON, CANADA N6B 5A7; bhart7@uwo.ca

Abstract—Although exposed around the margins of the San Juan Basin, Upper Cretaceous rocks of northwestern New Mexico were deposited in a much larger predecessor basin that owes its origin to the breakup of Pangea and an acceleration of Mid-Atlantic Ridge spreading rates. This paper presents a high-level overview of the Upper Cretaceous Western Interior Seaway, an inland sea that extended from the current Gulf of Mexico to the Arctic Ocean and from Utah to Kansas. I link deposits exposed in the San Juan Basin area with time-equivalent rocks deposited elsewhere in the Western Interior Seaway to illustrate the extent of the seaway and controls on sediment deposition.

Westward movement of North America, initiated in the Jurassic, accelerated during the Late Cretaceous. Retroarc foreland basins along the western margin of the continent deepened. Flat-slab subduction created dynamic topography that widened the basin. At the same time, mid-ocean ridge swelling raised eustatic sea level. That combination of subsidence and eustasy led to the formation of the Western Interior Seaway. Upper Cretaceous rocks of New Mexico and elsewhere record a relatively rapid flooding of the basin during the Cenomanian followed by a more gradual retreat of the seaway throughout the rest of the Cretaceous. Superimposed on that second-order trend were third-order transgressive-regressive cycles formed in response to shorter-term (tens of thousands to millions of years) fluctuations in subsidence, eustatic sea level, and sediment supply. That combination of short- and long-term cyclicity explains stacking patterns and facies transitions associated with the Dakota and Gallup sandstones, Mesaverde Group, and other Upper Cretaceous units in New Mexico and elsewhere in North America's interior.

INTRODUCTION

Upper Cretaceous rocks are exposed around the margins of the San Juan Basin (Figs. 1 and 2). But they were deposited in a much more extensive basin before the San Juan Basin formed. These rocks are marine sandstones, shales, and calcareous deposits of the Cretaceous Western Interior Seaway and associated nonmarine strata that were deposited landward of a contemporaneous shoreline. At its peak, the Western Interior Seaway extended from the current Gulf of Mexico to the Arctic Ocean, and eastward from Utah and British Columbia to Missouri and Manitoba (Fig. 3).

The San Juan Basin is mostly a Paleogene feature that deformed Upper Cretaceous and older units deposited in completely different basin settings. It is one of several Cenozoic basins in the Rocky Mountains area that deformed and preserved Upper Cretaceous strata (Lawton, 2019). Aspects of the polyphase tectonic history of the San Juan Basin and adjacent areas were summarized by Yonkee and Weil (2015), Lawton (2019), and Hart (2021), and will not be repeated here.

This paper provides a brief overview of the Cretaceous Western Interior Seaway, its formation, its history of sea-level change, and how that change is preserved in the stratigraphic record. The intent is to provide continent-scale context to help understand the formation and characteristics of Upper Cretaceous rocks exposed along the eastern margin of the San Juan Basin. Hart (2021) summarized petroleum systems and production from Upper Cretaceous and other rocks in the San Juan Basin, a major source of natural gas with relatively minor oil production.

THE CRETACEOUS WESTERN INTERIOR SEAWAY

The idea that much of central North America was covered by a seaway in the Cretaceous dates to the middle of the 19th century. By the early 20th century, it was understood that the seaway had experienced multiple episodes of growth and that contraction of that seaway had occurred (Waage, 1975). Kauffman (1977) defined successive episodes of transgression and regression (T-R cycles) for the North American interior during the Cretaceous, each lasting several million years. Peter Vail and coworkers at Exxon introduced concepts of seismic stratigraphy (Vail et al., 1977), later to become sequence stratigraphy, in that same year. The extent to which T-R cycle (or "sequence") development is driven by global changes in sea level continues to be debated.

Kauffman and Caldwell (1993) defined nine significant T-R cycles for the Cretaceous, four of which occur in the Late Cretaceous. Each T-R cycle lasted several million years, and it was superimposed on a long-term trend lasting approximately 36 million years (Fig. 4). That long-term trend began at the start of the Cenomanian, reached a maximum transgression in the early Turonian, and was followed by a more gradual regression throughout the rest of the Late Cretaceous. Kauffman and Caldwell (1993) suggested that higher frequency changes (hundreds of thousands of years) are superimposed on some parts of the curve. Similar orders of nested cyclicity have been proposed for eustatic changes in the Cretaceous (e.g., Haq, 2014) and at other times.

The veracity of Kauffman and Caldwell's (1993), Haq's (2014), or similar curves depends on the strength of biostratigraphic correlations from disparate parts of the basin or globe, and the plausibility of forcing mechanisms. Globally

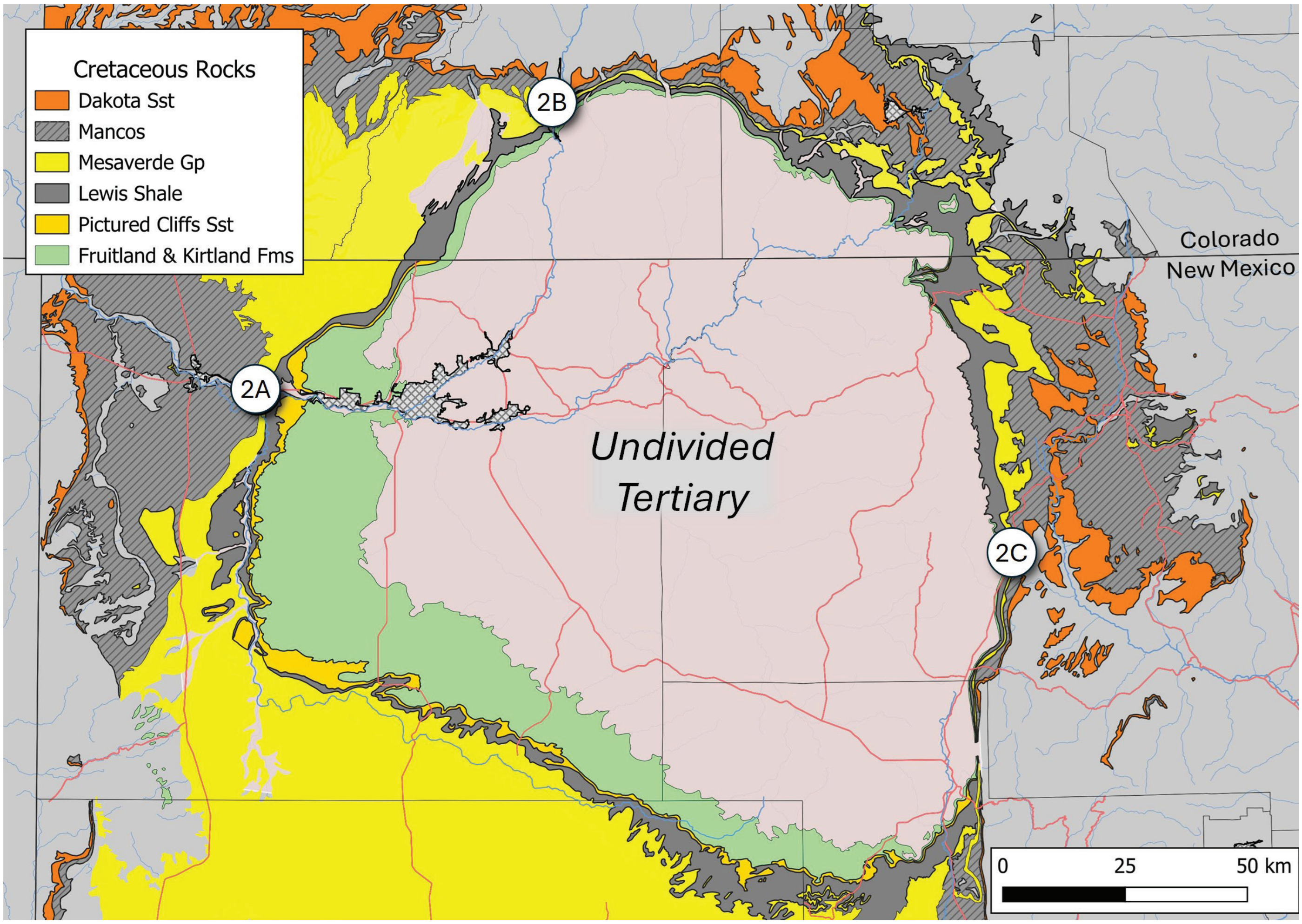

Figure 1. Simplified geologic map of the San Juan Basin highlighting primary Upper Cretaceous units around the margins. Numbers indicate locations of outcrops shown in Figure 2.

synchronous transgressions and regressions lasting tens or hundreds of millions of years are relatively easy to demonstrate and explain as being tectonically driven. Similarly, eustatic changes lasting tens to hundreds of thousands of years are known from the Quaternary and other times in Earth's past and can be attributed to glaciations. The recurring challenge is whether T-R cycles (or sequences) lasting a few million years can be attributed to eustasy, at least in part, because potential driving mechanisms remain elusive (e.g., Davies and Simmons, 2023).

Cretaceous Western Interior Seaway: Drivers of T-R Cycles

The mechanisms responsible for generating T-R cycles in sedimentary basins are relatively simple to understand once the term accommodation is defined. Accommodation refers to the space available for sediment to accumulate. It is the product of three factors: vertical crustal movements (subsidence and uplift), eustasy, and sediment supply (Jervey, 1988; Fig. 5). In marine settings like the Western Interior Seaway, the interplay among these three variables causes transgressions and regressions. When sediment supply exceeds the rate at which accommodation is generated, the shoreline progrades (regression). When sediment supply is less than the rate at which accommodation is generated, the shoreline is pushed landward (transgression).

Four factors contributed to the formation of the Western Interior Seaway and its fill. The first involves flexural subsidence (basin formation) in response to supracrustal loading by thrust sheets. This is the mechanism associated with the formation of foreland basins. With the breakup of Pangea, North America's western edge became a convergent margin. The (mostly) Cretaceous Sevier orogeny transported older passive-margin deposits eastward as a series of thrust sheets that loaded the crust (Yonkee and Weil, 2015), leading to the development of retroarc foreland basins of varying sizes and durations, extending from Arizona several thousand kilometers northward to British Columbia, Canada.

The west-east width of the Western Interior Seaway cannot be explained simply by subsidence due to flexural loading because the basin is too wide (Fig. 6). A second mechanism must have been active to generate such widespread subsidence, as noted by Cross and Pilger (1978). This mechanism is thought to be dynamic topography, a term that refers to vertical crustal movements occurring in response to mantle flow. Cold subducting slabs form positive mass anomalies that generate viscous mantle flow that, in turn, leads to vertical crustal movements (Burgess, 2019). Low-angle (flat-slab) subduction of the Farallon plate during the Late Cretaceous is thought to have generated, through associated dynamic topography, subsidence that extended far eastward (e.g., into Kansas and beyond) beneath the North American craton (Yonkee and Weil, 2015; Burgess, 2019).

Eustasy (global sea-level change) contributed to the shrinking and growth (via creation and removal of accommodation) of the Western Interior Seaway throughout the Late Cretaceous. Spreading rates of the Mid-Atlantic Ridge were high during much of the Late Cretaceous (e.g., Pitman, 1978; Seton et al., 2009). The rapid formation of young, low-density oceanic crust caused the mid-ocean ridge to swell, and water was displaced from the ocean basins onto continental crust. This is the only feasible process for generating eustatic changes of hundreds of meters (Conrad, 2013), and most reconstructions of Phanerozoic sea-level change suggest that global sea level was at its peak (approximately 250 m above present-day mean sea level) near the Cenomanian-Turonian boundary (Haq, 2014). As noted previously, the possibility of eustatic changes lasting a few million years remains debated. Finally, flooding of the continental interior, in response to the flexural loading, dynamic topography, and eustasy, enhanced broad-scale subsidence because of the associated isostatic response.

All three types of subsidence, and eustatic rises, generate accommodation into which sediment can be deposited. During the Late Cretaceous, much of the Western Interior Seaway's sediment fill was supplied by erosion of uplifted areas

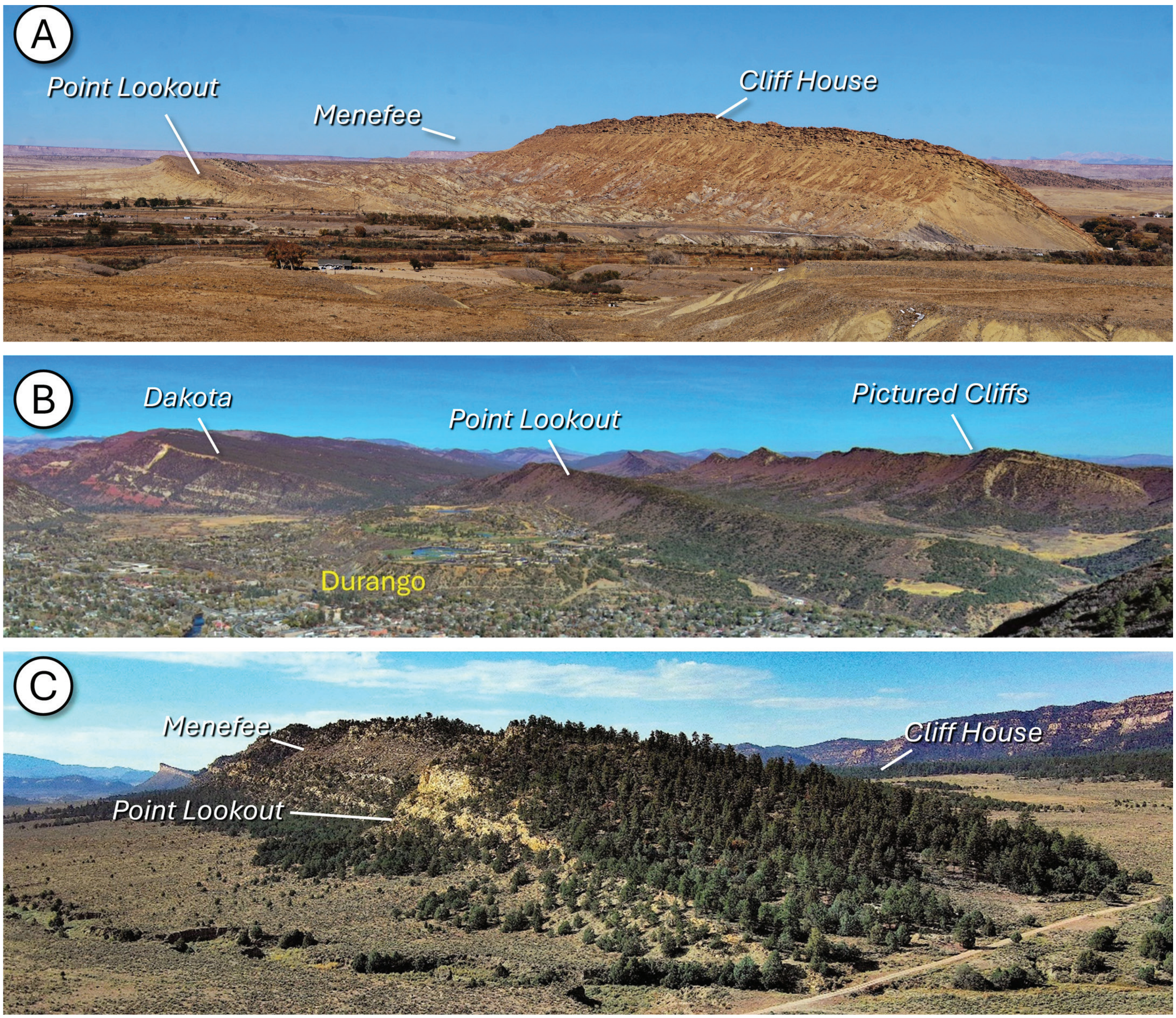

Figure 2. Outcrops of Upper Cretaceous deposits around the northern periphery of the San Juan Basin. A: Mesaverde Group (Point Lookout Sandstone, Menefee Formation, and Cliff House Sandstone) exposed on the Hogback monocline along U.S. Route 64 west of Farmington, NM. View to north. B: Sandstones of the Dakota, Point Lookout, and Pictured Cliffs formations form prominent ridges east of Durango, CO. View to east. C: The Mesaverde Group forms a prominent cuesta north of Llaves, NM. View to south. Locations of all outcrops shown on Figure 2 and provided in Table 1.

in fold-thrust belts along the western margin of the seaway. Eustatic changes would have affected the entire Western Interior Seaway simultaneously, but the location of fold-thrust belts varied in both time and space along the western continental margin. Therefore, patterns of subsidence and rates of sediment supply varied spatially throughout the duration of the Western Interior Seaway. Synchronous transgressions and regressions may have occurred in some parts of the basin, and at some times and over some timescales, but not at others.

Stratigraphy of the Upper Cretaceous Western Interior Seaway in New Mexico and Beyond: A Quick Tour

Despite ongoing debates about the role of eustatic changes lasting tens of thousands to millions of years in the Late Cretaceous, the broad history of T-R cycles depicted in Figure 4 is not seriously challenged. This section provides a high-level review of those cycles throughout the Western Interior Seaway and links them to Upper Cretaceous stratigraphy of the San Juan Basin and adjacent areas. For reference, Figure 7A presents a southwest-northeast stratigraphic cross section through the Upper Cretaceous section of the San Juan Basin that is simplified from Molenaar et al. (2002). Figure 8 shows wireline logs from a well that penetrates the entire Upper Cretaceous succession in the north-central part of the basin. The long-term (second-order in current sequence stratigraphic usage) cycle begins with transgression in the Cenomanian followed by regression throughout the rest of the Late Cretaceous. Superimposed on that long-term trend are shorter duration (third-order cycles lasting a few million years; Fig. 7B) T-R cycles that correspond to prominent formations and groups and include prograding shallow marine sandstones of the Gallup Sandstone, Point Lookout Sandstone, and Pictured Cliffs Sandstone. Sandstones associated with transgression include those of the Dakota Sandstone and Cliff House Sandstone. Further

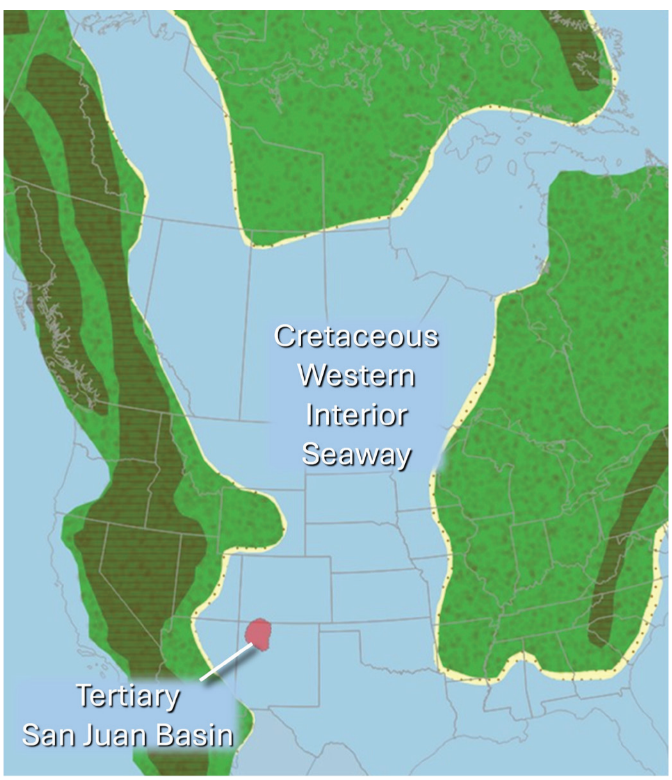

Figure 3. Schematic representation of the Western Interior Seaway at its maximum extent ~94 Ma near the Cenomanian-Turonian boundary. Green areas represent land, yellow areas represent shoreline deposits, and blue represents inundated areas. Red area shows (for reference) the extent of the Cenozoic San Juan Basin, a structural feature that had not yet formed in the Late Cretaceous. Redrawn and modified from Kauffman and Caldwell (1993).

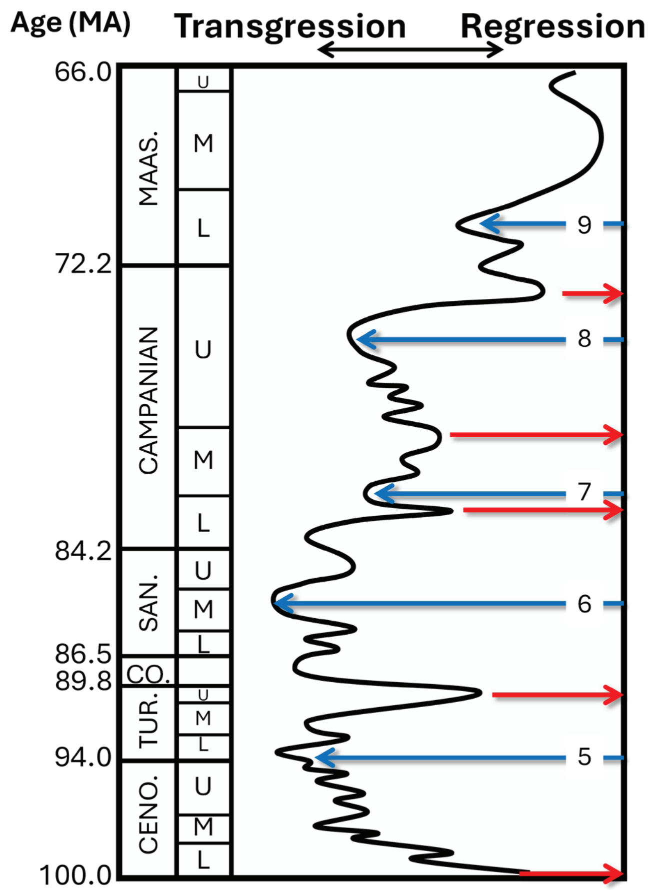

Figure 4. Relative sea-level chart for the Western Interior Seaway in the Late Cretaceous, redrawn from Kauffman and Caldwell (1993). The section is divided into stages (bottom to top: Cenomanian, Turonian, Coniacian, Santonian, Campanian, Maastrichtian) that are, in turn, divided into lower, middle, and upper substages. Black line illustrates reconstructed shoreline movements presumed to be basin wide. Colored arrows defined nine major transgressive-regressive cycles for the Upper Cretaceous. Red arrows indicate times of maximum regression (i.e., the minimum extent of the Western Interior Seaway) and numbered blue arrows indicate times of maximum transgression (i.e., the maximum extent of the Western Interior Seaway). Note the suggestion of even shorter duration T-R cycles. Ages of stage boundaries from Singer et al. (2023).

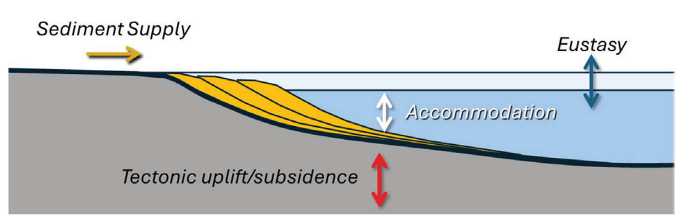

Figure 5. Simplified depiction of the interplay among tectonic subsidence/uplift, eustasy, and sediment supply to control accommodation; e.g., the space available for sediment to accumulate.

details of the Upper Cretaceous stratigraphy were summarized by Hart (2021).

Outcrops around the margins of the San Juan Basin expose portions of the Upper Cretaceous section (Fig. 2). The entire section is continuous and partially exposed in the Durango area in southwest Colorado although thick shale-dominated parts of the section are generally poorly exposed (but see Nelson and Sonnenberg, 2021). The interval between the Cenomanian Dakota Sandstone and Campanian Point Lookout Sandstone is variably exposed south and west of El Vado Reservoir (Fig. 9). Leckie et al. (1997) documented the stratigraphy of that same interval along the northwest basin margin near Point Lookout in southwest Colorado. The Upper Cretaceous section above the Cliff House Sandstone tends to be poorly exposed. An exception is in the area of the Bisti Badlands (south of Farmington, New Mexico) where nonmarine rocks of the Fruitland and Kirtland formations are exposed.

In the discussion that follows, most examples of shallow-marine sandstones are from the western margin of the Western Interior Seaway where strata were preserved because of relatively rapid subsidence. The eastern margin of the seaway, potentially running from Arkansas into Ontario, is much more poorly characterized because subsidence rates were not high enough to preserve Late Cretaceous shorelines.

TABLE 1. Locations of all outcrops shown in figures.

Figure	Locality	Longitude	Latitude
Figure 1	Hogback Monocline	−108.5409	36.7463
Figure 1	Durango	−107.9036	37.2625
Figure 1	Llaves	−106.8188	36.4286
Figure 9	El Vado Reservoir	−106.7990	36.5580
Figure 10	I-70	−105.2019	39.7022
Figure 11	Tierra Amarilla	−106.8344	35.5021
Figure 13	Grand Staircase	−111.6500	37.0814
Figure 13	Pueblo	−104.7321	38.2819
Figure 13	Wilson Dam	−98.5058	38.9657
Figure 13	El Vado Reservoir	−106.7444	36.6472
Figure 13	Vermillion River	−100.1431	51.0620
Figure 13	Ram Falls	−115.8269	52.0920
Figure 13	Fite Ranch	−106.7534	33.8848
Figure 14	Mistanusk Creek	−120.0860	54.6693
Figure 14	Gaudalupe Ruin	−107.1263	35.5181
Figure 14	Wall Creek	−106.5691	43.6068
Figure 15	Monument Rocks	−100.7640	38.7954
Figure 15	Langtry	−101.6257	29.8296
Figure 18	Point Lookout	−108.4180	37.3160
Figure 18	Hatch Mesa	−109.9370	38.9460
Figure 18	Wyoming	−109.0899	41.7991
Figure 18	El Vado Reservoir	−106.7280	36.5828
Figure 19	Coal Canyon	−108.3997	39.1382

The focus of this paper is primarily on the Upper Cretaceous section (i.e., Cenomanian and younger), but the Western Interior Seaway first connected the Arctic Ocean with Tethys Ocean in the Albian. This seaway is known as the Skull Creek Seaway (Kauffman, 1977; Blakey, 2014), but there are no strata of this age preserved in New Mexico. In the northern plains states and southern Canadian Prairie Provinces, some of this time interval is represented by the Joli Fou Shale and associated shallow-marine formations such as the Viking Formation (Mossop and Shetsen, 1994). An outcrop along Interstate 70 west of Denver exposes Albian nonmarine and shallow-marine rocks of the Dakota Group that are unconformably overlying the Jurassic Morrison Formation (Fig. 10). Note that the Dakota has Group status here, as it does in Nebraska where the Dakota was originally defined.

The Western Interior Seaway began flooding the continental interior in the early Cenomanian, following a regression at the Albian–Cenomanian boundary, and eventually rejoined the Arctic and Tethys Oceans. Flooding pushed the shoreline towards the basin margin and, in so doing, preserved transgressive sandstones assigned to the Dakota Sandstone in New Mexico. These sandstones are younger than the Dakota Group to the east. They were called Dakota because they (lithostratigraphically) resemble the Dakota Group east of the Rockies and occupy a similar stratigraphic position, unconformably overlying the Jurassic Morrison Formation. Chronostratigraphically, the Dakota Sandstone is time equivalent to the Graneros Shale farther east (e.g., in the Denver Basin).

In the San Juan Basin and adjacent areas, the Dakota Sandstone is overlain by and interfingers with marine shales of the lower Mancos Shale suggesting the broad-scale Cenomanian transgression was punctuated by relatively short-lived regressions (Fig. 11). The Dakota Sandstone becomes even younger westward, towards the Western Interior Seaway margin because of the time-transgressive nature of sedimentation. In Utah, facies-equivalent strata are assigned to the Naturita Formation and Mancos-equivalent shales are assigned to the Tropic Shale (Fig. 12).

The westward translation of the shoreline, largely in response to the mid-Cretaceous eustatic rise driven by accelerated spreading at mid-ocean ridges, was accompanied by

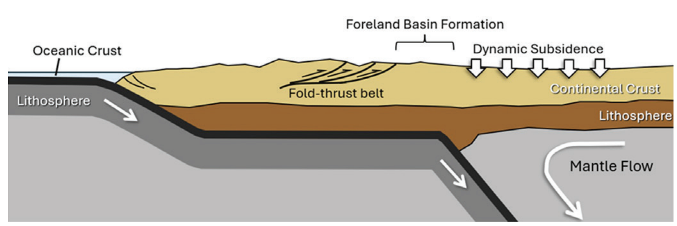

Figure 6. Schematic representation of flat-slab subduction and associated subsidence patterns. Lateral shortening leads to development of a fold-thrust belt that generates a relatively narrow foreland basin. Subduction of cold lithosphere hundreds of kilometers inboard of the continental margin generates mantle flow that leads to subsidence of a broad zone (dynamic topography).

increased foreland-basin subsidence and led much of the basin to be represented by offshore shales. These fine-grained deposits include the Mancos Shale in the Southwest and the shales of the Colorado Group in more northern areas, including the southern Prairie Provinces of Canada.

A eustatic highstand occurred in the earliest Turonian (~94 Ma), with mean sea level ~250 m higher than present (Haq, 2014). This corresponds to T5 in Figure 4. With shorelines pushed landward, the basin center became relatively starved of siliciclastic sediment and much of the sediment delivered to the sea floor consisted of the calcareous remains of planktonic organisms such as coccoliths (i.e., the marlstones and limestones in Fig. 13). Hart (2016) presented a process-based depositional model for the Western Interior Seaway at this time. In New Mexico, the shoreline was pushed southwestward, probably outside the current state boundary, allowing calcareous deposits to accumulate in the area of the Cookes

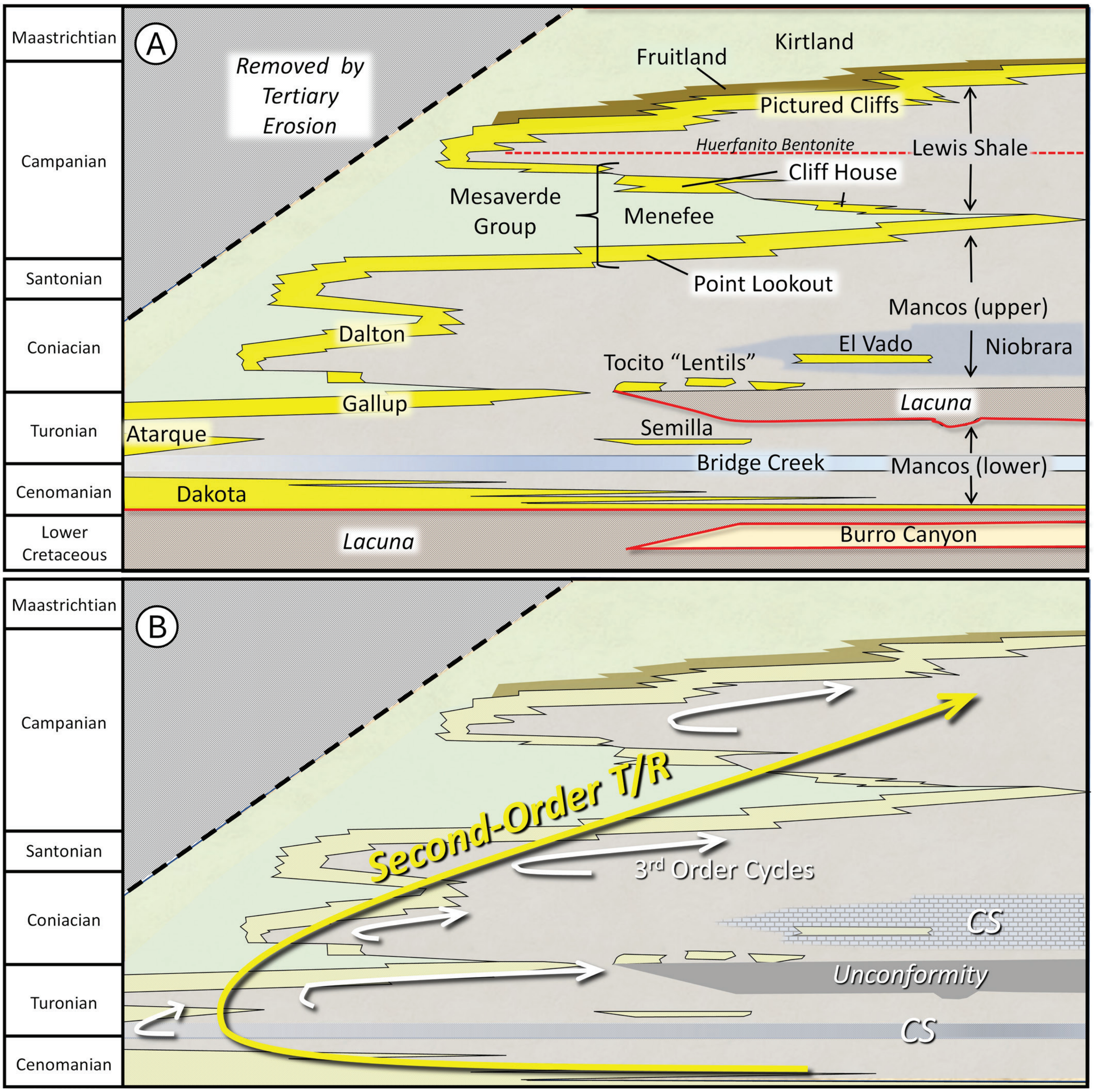

Figure 7. A: Cretaceous stratigraphy in the San Juan Basin area, shown as a SW–NE (left-right) cross section. Gray areas are marine shale, yellow areas are shoreline sandstones, green areas are nonmarine deposits, brown area depicts the Fruitland Coal, and blue areas are calcareous marine deposits. Hachured areas represent missing strata (erosion or nondeposition). Based on Molenaar et al. (2002). B: The same cross section as in A, showing relative sea-level trends. A second-order (tens of millions of years) transgression/regression (T-R cycle) is shown by the yellow curve, and white curves represent third-order cycles lasting a few million years. Condensed sections (CS) are times when siliciclastic sediment supply was reduced to the basin and sediments are calcareous. Compare with transgressions and regressions depicted in Figure 4.

Range, north of Deming (Hook and Cobban, 2015).

The Cenomanian-Turonian boundary interval in the center of the Western Interior Seaway is represented by interbedded limestones and calcareous shales (Figs. 14A–14C). Similar facies are present in the time-equivalent Upper Eagle Ford Formation at the southern margin of the Western Interior Seaway (Hart et al., 2020). The lithologic alternations are thought to be the product of tens-to-hundreds-of-thousands-year climate cycles (now known as Milankovitch cycles), an idea first proposed by Gilbert (1895). Primary productivity was highest in the southern part of the Western Interior Seaway and time-equivalent rocks in Canada tend to be less calcareous and lack the dm-scale limestone beds (Fig. 14D). The interval also becomes more siliciclastic towards the western margin of the basin; i.e., towards the sources of siliciclastic sediment (Figs. 14E and 14F).

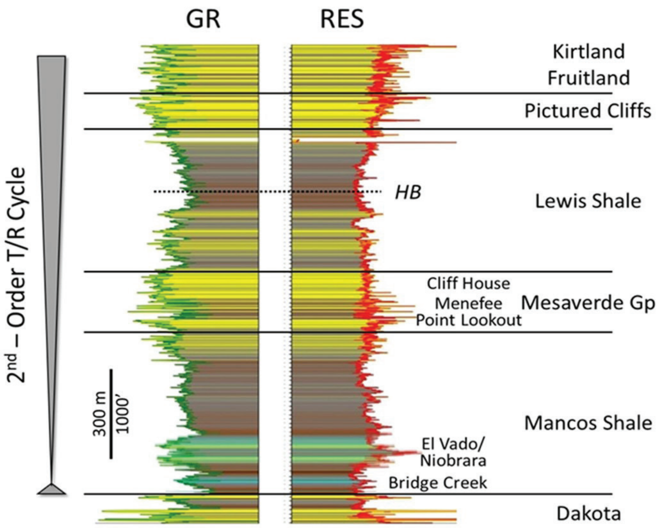

Figure 8. Wireline logs showing Upper Cretaceous stratigraphy in the north-central part of the San Juan Basin (Williams Rosa Unit 29A, 32-32N-6W, API: 30-045-11136). Gamma-ray (GR) log at left and resistivity (RES) log at right. This combination of logs is commonly used to depict subsurface stratigraphy. Colored curve fill is based on the GR log: yellow is sandstone, brown is shale, and blue is calcareous. Gray arrows at the far left show interpreted long-term (second-order) trend of transgression and regression. Triangle at base represents a relatively short transgression, with peak transgression represented by the Bridge Creek Limestone. Inverted triangle represents a long-term regression.

Near the end of the Turonian (~90 Ma) an abrupt, high-magnitude sea-level fall caused siliciclastic shorelines to prograde into the basin (Fig. 15). In New Mexico, this time is associated with deposition of the Gallup Sandstone. Farther north, this corresponds to the Wall Creek and Turner Sandstones in Wyoming. Even farther north, in Alberta and northeast British Columbia, this shoreline progradation is represented by the Cardium Formation (Mossop and Shetsen, 1994).

A significant unconformity separates Turonian strata from Coniacian strata throughout much of the Western Interior Seaway. This hiatus was termed the Carlile-Niobrara unconformity in western Kansas (Hattin, 1962) and the Basal Niobrara unconformity in the San Juan Basin area (Bottjer and Stein, 1994) where its formation was attributed to local tectonic movements (McCubbin, 1969). A time-equivalent unconformity is present between the Upper Eagle Ford Formation and Austin Chalk in south Texas (Denne et al., 2016) and within the Cardium Formation of Alberta (Plint et al., 2022). The origin of an unconformity that appears to stretch from Alberta to south Texas and east into Manitoba and Kansas remains problematic.

Sea level was high throughout much of the Coniacian and Santonian (~90–84 Ma; Fig. 4) with shorelines generally pushed far towards the basin margin. The Dalton Sandstone of the San Juan Basin was deposited at this time during a relatively short-lived regression. The basin center once again

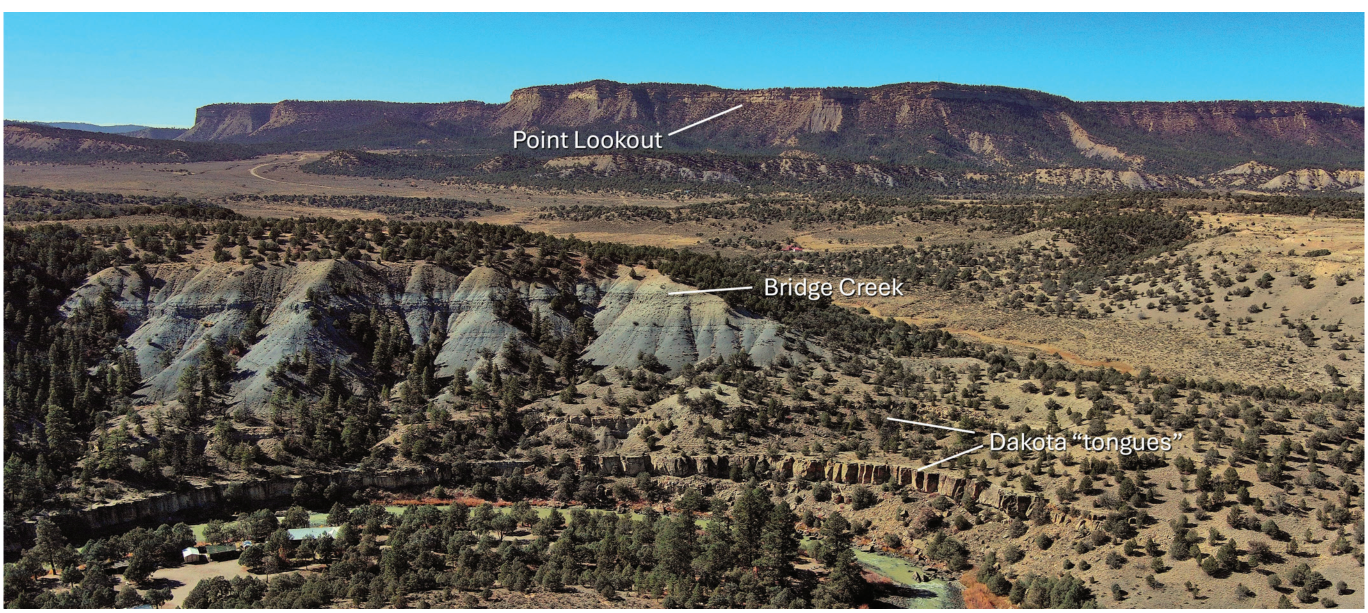

Figure 9. Drone-based overview of part of the Upper Cretaceous section in north-central New Mexico. The Dakota Formation at the base of the section formed during the Cenomanian flooding of the Western Interior Seaway. Limestones and calcareous shales of the Bridge Creek Limestone represent peak highstand near the Cenomanian–Turonian boundary (~94 Ma). The cliff-forming Point Lookout Sandstone (in the distance) formed during an early Campanian regression. Compare with Figures 7 and 8. Outcrop location provided in Table 1.

became starved of siliciclastic sediments and became a location where the remains of calcareous organisms dominated the sediment supplied to the sea floor. This relatively prolonged period (~5 million years) led to deposition of the Niobrara Chalk in the basin center, and Austin Chalk at the southern end of the Western Interior Seaway (Fig. 16). More siliciclastic shales (generally not well exposed) were deposited where clastic influx was higher. These include the upper Mancos Shale in New Mexico (Nelson and Sonnenberg, 2021) and the First White Specks Formation in Canada.

Shorelines began to prograde towards the basin center in the early Campanian (~84 Ma; Figs. 4 and 17). This progradation is represented in the Mesaverde Group of the southwest part of the Western Interior Seaway (Fig. 18). It corresponds to the Point Lookout Sandstone in the San Juan Basin area, the Grassy, Desert and other members of the Blackhawk Formation in the Book Cliffs area of central Utah, and other time-equivalent rocks in Wyoming. In southern Alberta, this progradation is expressed in the Chungo Member of the Wapiabi Formation (Mossop and Shetsin, 1994). The sedimentology and stratigraphy of the Mesaverde Group in New Mexico are examined in greater detail in Hart (this volume).

A final mid-Campanian flooding of the northern New Mexico area is represented by the Lewis Shale in the San Juan

Figure 10. Outcrop west of Denver on I-70 (Dakota hogback) showing Albian strata of the Dakota Group (left) unconformably overlying the Jurassic Morrison Formation (right). Unconformity indicated by the dashed yellow line. The Dakota consists mostly of nonmarine and shallow-marine deposits at this location. Rocks of this age are not preserved in the San Juan Basin. Outcrop location provided in Table 1.

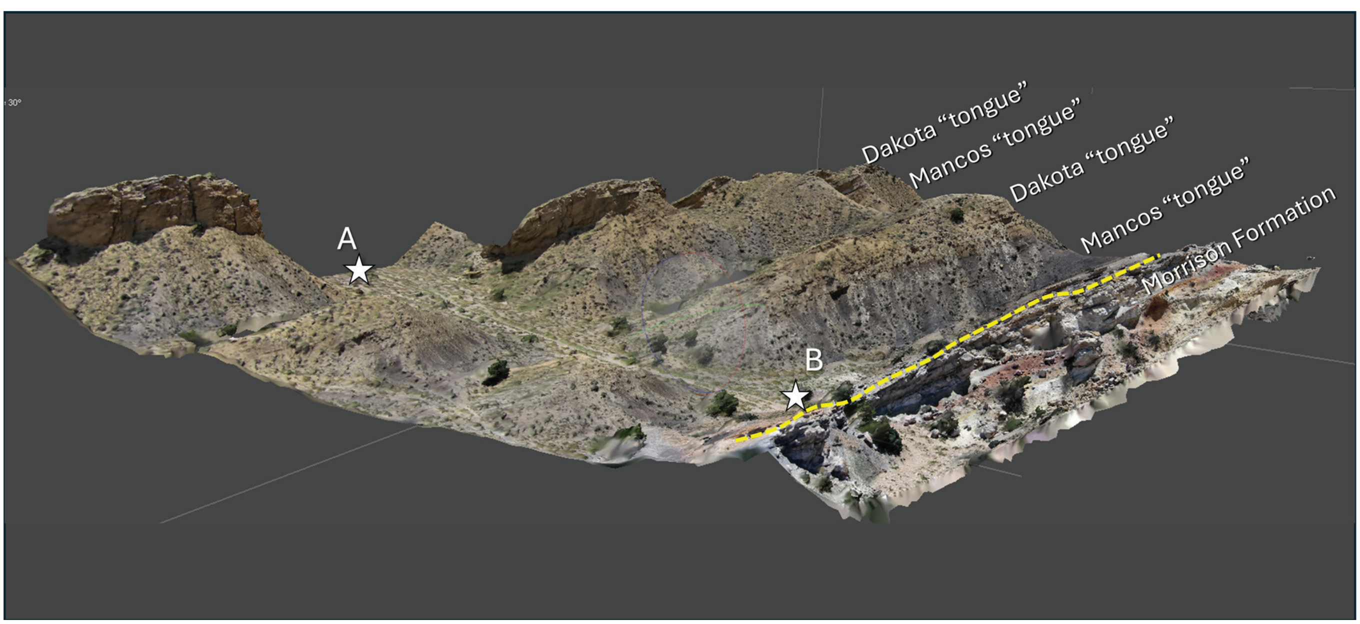

Figure 11. Drone-based 3D model of an outcrop at the south end of the Tierra Amarilla anticline showing the unconformable contact (yellow dashed line) between the Jurassic Morrison Formation and the overlying Cenomanian section of interfingering tongues of Mancos Shale and Dakota Sandstone. Distance along the trail between points A and B is approximately 80 m. Outcrop location provided in Table 1.

Figure 12. Stratigraphic transition between shallow-marine sandstones of the Upper Cenomanian Naturita Formation (broadly equivalent to the Dakota Sandstone) and the overlying Tropic Shale (broadly equivalent to the Mancos Shale) at Grand Staircase-Escalante National Monument in south-central Utah. Outcrop location provided in Table 1.

Basin area with latest Campanian regression, and final retreat of the Western Interior Seaway in that area represented by progradation of the Pictured Cliffs Sandstone (Molenaar et al., 2002; Fig. 19). This regression is approximately the same age as the regression defined by the Isles Formation several hundred kilometers to the north, in the Piceance Basin of Utah and western Colorado (Robinson Roberts and Kirschbaum, 1995; Minor et al., 2022). Both the Pictured Cliffs Sandstone and Isles Formation are overlain by coal-bearing rocks (Fruitland Coal and Cameo-Wheeler coal zone respectively) deposited landward of the prograding shoreline. Importantly, because of miscorrelation, the Lewis Shale of the San Juan Basin is 2–4 million years older than the Lewis Shale farther north in Wyoming and Colorado. The latter represents the final transgression of the Western Interior Seaway in the latest Campanian and early Maastrichtian (Minor et al., 2022) and is equivalent to the Bearpaw Shale even farther north in Montana and Canada. There are no time-equivalent marine rocks in northern New Mexico.

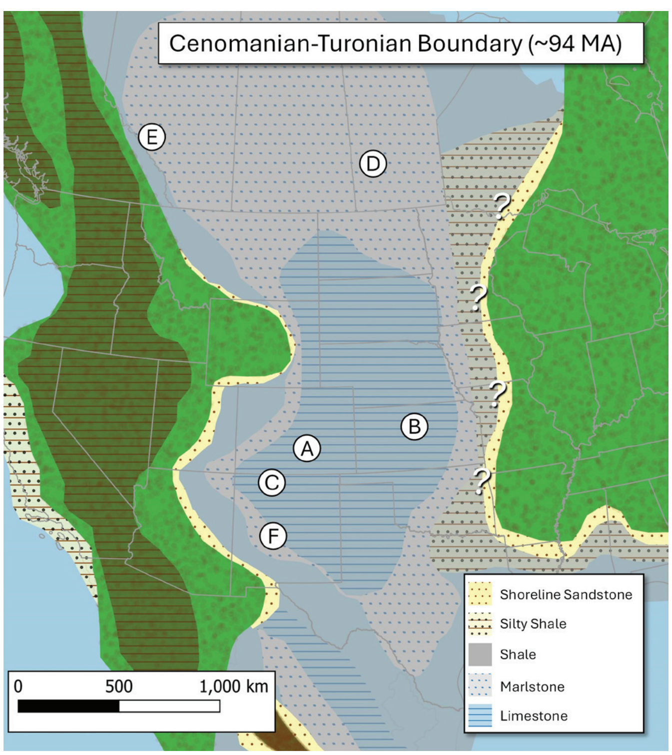

Figure 13. Schematic representation of Western Interior Seaway paleogeography at peak eustatic highstand near the Cenomanian–Turonian boundary. Green areas are land. Redrawn and modified from Kauffman and Caldwell (1993). The location of the eastern shoreline is speculative because it is not preserved. Lettered circles show locations of outcrops shown in Figure 15.

SUMMARY

The San Juan Basin is a Cenozoic feature that exposes Upper Cretaceous rocks around its margin and preserves them in the subsurface of the basin center. These Cretaceous strata were deposited in, and landward of, a seaway that extended from the current Gulf of Mexico (the then Tethys Ocean) to the Arctic Ocean and, at its peak extent, from Utah to Kansas and beyond. The Western Interior Seaway predates the San Juan Basin.

Ultimately, the growth and demise of the Western Interior Seaway was driven by the breakup of Pangea. Westward movement of the North American craton, in response to the opening of the Atlantic Ocean, led the western cratonic boundary to become a convergent margin several thousand kilometer in length. Foreland basins formed to the east of the orogenic belt. Flat-slab subduction beneath the continent generated dynamic topography that extended subsidence far eastward of the foreland basins. A pulse of mid-ocean ridge growth in the Late Cretaceous raised global sea level by as much as 250 m above present-day levels. This combination of subsidence and eustatic highstand led to the flooding of the continental interior and the formation of the Western Interior Seaway. Although broad-scale correlations of T-R cycles lasting millions of years can be defined in different parts of the basin, not all such cycles, or shorter-duration cycles, can be correlated. These differences probably reflect variability in tectonic subsidence and sediment supply throughout and around the basin.

Outcrops of Upper Cretaceous rocks representing different parts of the Western Interior Seaway at different times help illustrate a transgressive-regressive cyclicity that has several temporal components. Flooding of the Western Interior Seaway began in the Albian. Following a significant regression at the Albian–Cenomanian boundary, the seaway again expanded and reached maximum dimensions near the Cenomanian–Turonian boundary, corresponding to the highest sea level of the Phanerozoic. The highstand was followed by a more gradual retreat of the seaway, punctuated by shorter term (of few million years duration) transgressive-regressive cycles of various magnitudes. Those shorter-term cycles are responsible for generating the shallow-marine sandstones (Dakota, Mesaverde, Gallup, Cardium, and others) that are widespread throughout the West in both the United States and Canada. During times of maximum transgression, at the Cenomanian–Turonian boundary and in the Coniacian–Santonian, the basin center became starved of siliciclastic sediment and calcareous deposits (remains of planktonic organisms) came to dominate.

REFERENCES

Blakey, R. C., 2014, Paleogeography and paleotectonics of the Western Interior Seaway, Jurassic–Cretaceous of North America—American Association of Petroleum Geologists Search and Discovery 30392: https://www.searchanddiscovery.com/pdfz/documents/2014/30392blakey/ndx_blakey.pdf.html (accessed December 28, 2016).

Bottjer, R. J., and Stein, J. A., 1994, Relationship of stratigraphic traps to submarine unconformities—Examples from the Tocito Sandstone, San Juan Basin, New Mexico and Colorado, *in* Dolson, J.C., Hendrick, M.I., Wescott, W.A., eds., Unconformity-related Hydrocarbons in Sedimentary Sequences, Guidebook for Petroleum Exploration and Exploitation in Clastic and Carbonate Sediments: Denver, Rocky Mountain Association of Geologists, p. 81–208.

Burgess, P.M., 2019, Phanerozoic evolution of the sedimentary cover of the North American craton, *in* Miall, A.D., ed., The Sedimentary Basins of the United States and Canada: Amsterdam, Netherlands, Elsevier, p. 39–75. https://doi.org/10.1016/B978-0-444-63895-3.00002-4

Conrad, C.P., 2013, The solid Earth's influence on sea level: Geological Society of America Bulletin, v. 125, p. 1027–1052. https://doi.org/10.1130/B30764.1

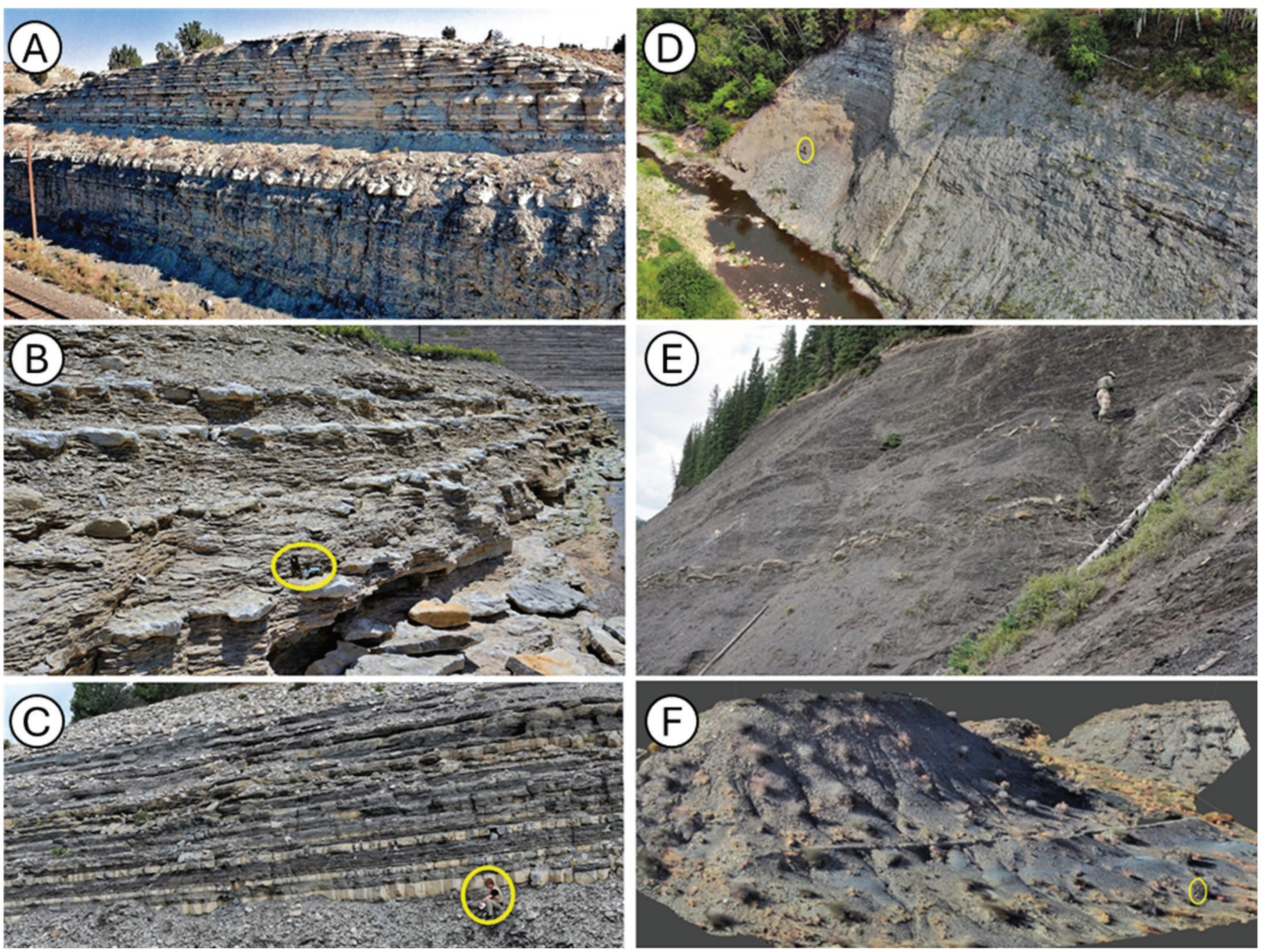

Figure 14. Lithologic characteristics of the Cenomanian-Turonian boundary section in various parts of the Western Interior Seaway. A: Interbedded limestones and marlstones west of Pueblo, CO. B: Interbedded limestones and marlstones at Wilson Dam in central Kansas. Keys (circled) for scale. C: Interbedded limestones and marlstones at the north end of El Vado Reservoir in north-central New Mexico. Drone pilot (circled) for scale. D: Marlstones from west-central Manitoba. Drone pilot (circled) for scale. E: Noncalcareous shales at Ram Falls in west-central Alberta. Person for scale. F: Drone-based outcrop model of calcareous shales with minor thin limestones at Carthage, NM. This interval corresponds to the interbedded limestones and shales shown in parts 14A–14C (Hook and Cobban, 2015). Spade ~45 cm long at lower right (circled) for scale. Locations of all outcrops shown on Figure 13. Outcrop locations provided in Table 1.

Cross, T. A., and Pilger, R. H., 1978, Tectonic controls of late Cretaceous sedimentation, western interior, USA: Nature, v. 274, p. 653–657. http://dx.doi.org/610.1038/274653a274650

Davies, A., and Simmons, M.D., 2023, Placing constraints on the nature of short-term eustatic curves: Basin Research, v. 36, e12832. https://doi.org/10.1111/bre.12832

Denne, R., Breyer, J., Callender, A., Hinote, R., Kariminia, M., Kosanke, T., Kita, Z., Lees, J., Rowe, H., Spaw, J., and Tur, N., 2016, Biostratigraphic and geochemical constraints on the stratigraphy and depositional environments of the Eagle Ford and Woodbine Groups of Texas, *in* Breyer, J. A., eds., The Eagle Ford Shale—A Renaissance in U.S. Oil Production: American Association of Petroleum Geologists, Memoir 110, p. 1–86. https://doi.org/10.1306/13541957M1103660

Gilbert, G.K., 1895, Sedimentary measurement of Cretaceous time: Journal of Geology, v. 3, p. 121–127.

Haq, B.U., 2014, Cretaceous eustasy revisited: Global and Planetary Change, v. 113, p. 44–58. https://doi.org/10.1016/j.gloplacha.2013.12.007

Hart, B.S., 2016, Marine mudstone source rocks in epicontinental basins—Development of a conceptual facies model and application to Cenomanian/Turonian mudstones of the Cretaceous Western Interior Seaway, *in*, Dolan, M., Higley, D., and Lillis, P., eds., Hydrocarbon Source Rocks in Unconventional Plays, Rocky Mountain Region: Denver, CO, Rocky Mountain Association of Geologists Special Publication, p. 1–58.

Hart, B.S., 2021, Stratigraphy and hydrocarbon resources of the San Juan Basin—Lessons for other basins, lessons from other basins: The Mountain Geologist, v. 58, p. 43–103. https://doi.org/10.31582/rmag.mg.58.2.43

Hart, B., Godet, A., Pope, M., and Griffith, C., 2020. Geologic controls on production, Upper Cretaceous Eagle Ford and Austin Chalk, South Texas: Tulsa, OK, Society of Sedimentary Geology Field Guidebook 16, 145 p. https://doi.org/10.2110/sepmfg.16

Hattin, D.E., 1962, Stratigraphy of the Carlile Shale (Upper Cretaceous) in Kansas: Kansas Geological Survey Bulletin 156, 155 p.

Hook, S.C., and Cobban, W.A., 2015, The type section of the Upper Cretaceous Tokay Tongue of the Mancos Shale (new name), Carthage coal field, Socorro County, New Mexico: New Mexico Geology, v. 37, p. 27–46. https://doi.org/10.58799/NMG-v37n2.27

Jervey, M.T., 1988, Quantitative geological modeling of siliciclastic rock sequences and their seismic expression, *in* Wilgus, C.K., Hasting, B.S., Kendall, C.G.St.C, Posamentier, HW, Ross, CA, and Van Wagoner, JC, eds., Sea-Level Changes—An Integrated Approach: Tulsa, OK, Society of Sedimentary Geology Special Publication 42, p. 47–69.

Kauffman, E.G., 1977, Geological and biological overview—Western Interior Cretaceous basin: The Mountain Geologist, 14, p. 75–99.

Kauffman, E., and Caldwell, W., 1993, The Western interior basin in space and time, *in* Caldwell, W., and Kauffman, E., eds., Evolution of the Western Interior Basin: Geological Association of Canada Special Paper 39, p. 1–30.

Koning, D.J., 2024, Comparison of the sedimentologic and stratigraphic characteristics of the Point Lookout vs. Gallup Sandstones near Cabezon, New Mexico: New Mexico Geological Society, Guidebook 74, p. 201–217. https://doi.org/10.56577/FFC-74.201

Lawton, T.F., 2019, Laramide sedimentary basins, *in* Miall, A.D., ed., The Sedimentary Basins of the United States and Canada: Amsterdam, Netherlands, Elsevier, p. 529–557. https://doi.org/10.1016/S1874-5997(08)00012-9

Leckie, R.M., Kirkland, J.I., and Elder, W.P., 1997, Stratigraphic framework and correlation of a principal reference section of the Mancos Shale (Upper Cretaceous), Mesa Verde, Colorado: New Mexico Geological Society, Guidebook 48, p. 163–216.

McCubbin, D.G., 1969, Cretaceous strike-valley sandstone reservoirs, northwestern New Mexico: American Association of Petroleum Geologists Bulletin, v. 53, p. 2114–2140. https://doi.org/10.1306/5D25C92B-16C1-11D7-8645000102C1865D

Minor, K.P., Steel, R.J., and Olariu, C., 2022, Tectonic and eustatic control of Mesaverde Group (Campanian–Maastrichtian) architecture, Wyoming-Utah-Colorado region, USA: Geological Society of America Bulletin, v. 134, p. 419–445. https://doi.org/10.1130/B36032.1

Molenaar, C.M., Cobban, W.A., Merewether, E.A., Pillmore, C.L., Wolfe, D.G., and Holbrook, J.M., 2002, Regional stratigraphic cross sections of Cretaceous rocks from east-central Arizona to the Oklahoma Panhandle: U.S. Geological Survey Miscellaneous Field Studies Map MF-2382.

Mossop, G.D. and Shetsen, I., (comp.) 1994, Geological atlas of the Western Canada Sedimentary Basin: Canadian Society of Petroleum Geologists and Alberta Research Council. https://ags.aer.ca/reports/atlas-western-canada-sedimentary-basin (accessed Jan 2, 2025).

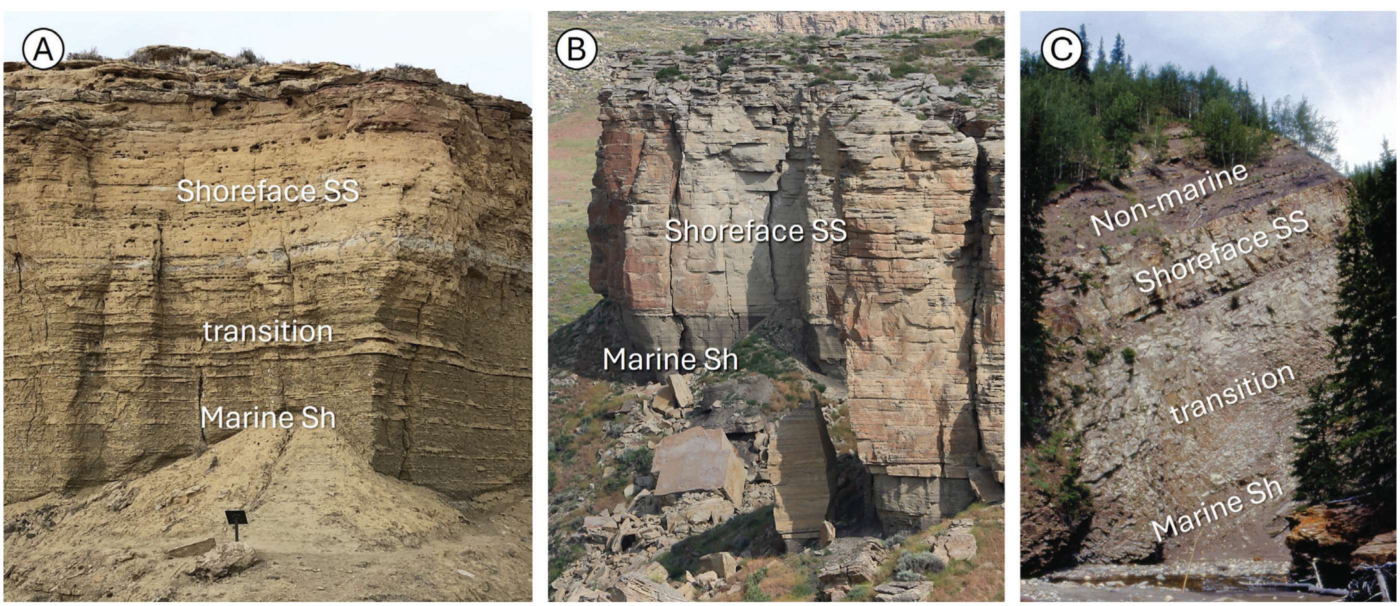

Figure 15. A: Outcrop of the Gallup Sandstone and underlying facies in central New Mexico, the Guadalupe Ruin section visited on the 2024 New Mexico Geological Society Fall Field Conference (Koning, 2024). Only the lowermost approximately 5 m of a >17-m-thick Gallup Sandstone shoreface sandstone is exposed in this outcrop (photo courtesy Dan Koning). B: Outcrop of the Upper Turonian Wall Creek Member of the Frontier Formation at the type locality in Wyoming (photo courtesy Michael Hofmann). C: Upper Turonian Cardium Formation at Mistanusk Creek in west-central Alberta. Cardium shoreface sandstones are ~20 m thick at this outcrop. Shoreface sandstones of the Gallup and Cardium gradationally overlie offshore shales whereas the contact between the Wall Creek and underlying marine shales is more abrupt. Outcrop locations provided in Table 1.

Nelson, W.W., and Sonnenberg, S.A., 2021, Sequence stratigraphy and regional context of the Mancos-Niobrara in the Northern San Juan Basin: The Mountain Geologist, v. 58, p. 105157. https://doi.org/10.31582/rmag.mg.58.2.105

Pitman, III, W.C., 1978, Relationship between eustacy and stratigraphic sequences of passive margins: Geological Society of America Bulletin, v. 89, p. 13891403. https://doi.org/10.1130/0016-7606(1978)89<1389:RBEASS>2.0.CO;2

Plint, A.G., Uličný, D., Čech, S., Walaszczyk, I., Gröcke, D.R., Laurin, J., Shank, J.A. and Jarvis, I., 2022, Trans-Atlantic correlation of Late Cretaceous high-frequency sea-level cycles: Earth and Planetary Science Letters, v. 578, 117323. https://doi.org/10.1016/j.epsl.2021.117323

Robinson Roberts, L.N., and Kirschbaum, M.A., 1995, Paleogeography of the Late Cretaceous of the Western Interior of middle North America—Coal distribution and sediment accumulation: U.S. Geological Survey Professional Paper 1561, 115 p.

Seton, M., Gaina, C., Müller, R.D., and Heine, C., 2009, Mid-Cretaceous seafloor spreading pulse—Fact or fiction?: Geology, v. 37, p. 687690. https://doi.org/10.1130/G25624A.1

Singer, B.S., Jicha, B.R., Sawyer, D.A., Walaszczyk, I., Landman, N., Sageman, B.R., and McKinney, K.C., 2023, A ^{40}A/^{39}A and U-Pb timescale for the Cretaceous Western Interior Basin, North America, *in* Hart, M.B., Batenburg, S.J., Huber, B.T., Price, G.D., Thibault, N., Wagreich, N., and Walaszczyk, I., eds., Cretaceous Project 200 Volume 1—The Cretaceous World: London, UK, Geological Society of London Special Publication, 544 p. https://doi.org/10.1144/SP544-2023-76

Vail, P.R., Mitchum, R.M., Jr., Todd, R.G., Widmier, J.M., Thompson, III, S., Sangree, J.B., Bubb, J.N., and Hatleilid, W.G., 1977, Seismic stratigraphy and global changes of sea level, *in* Payton, C.E., ed., Seismic Stratigraphy—Applications to Hydrocarbon Exploration: American Association of Petroleum Geologists Memoir 26, p. 49212.

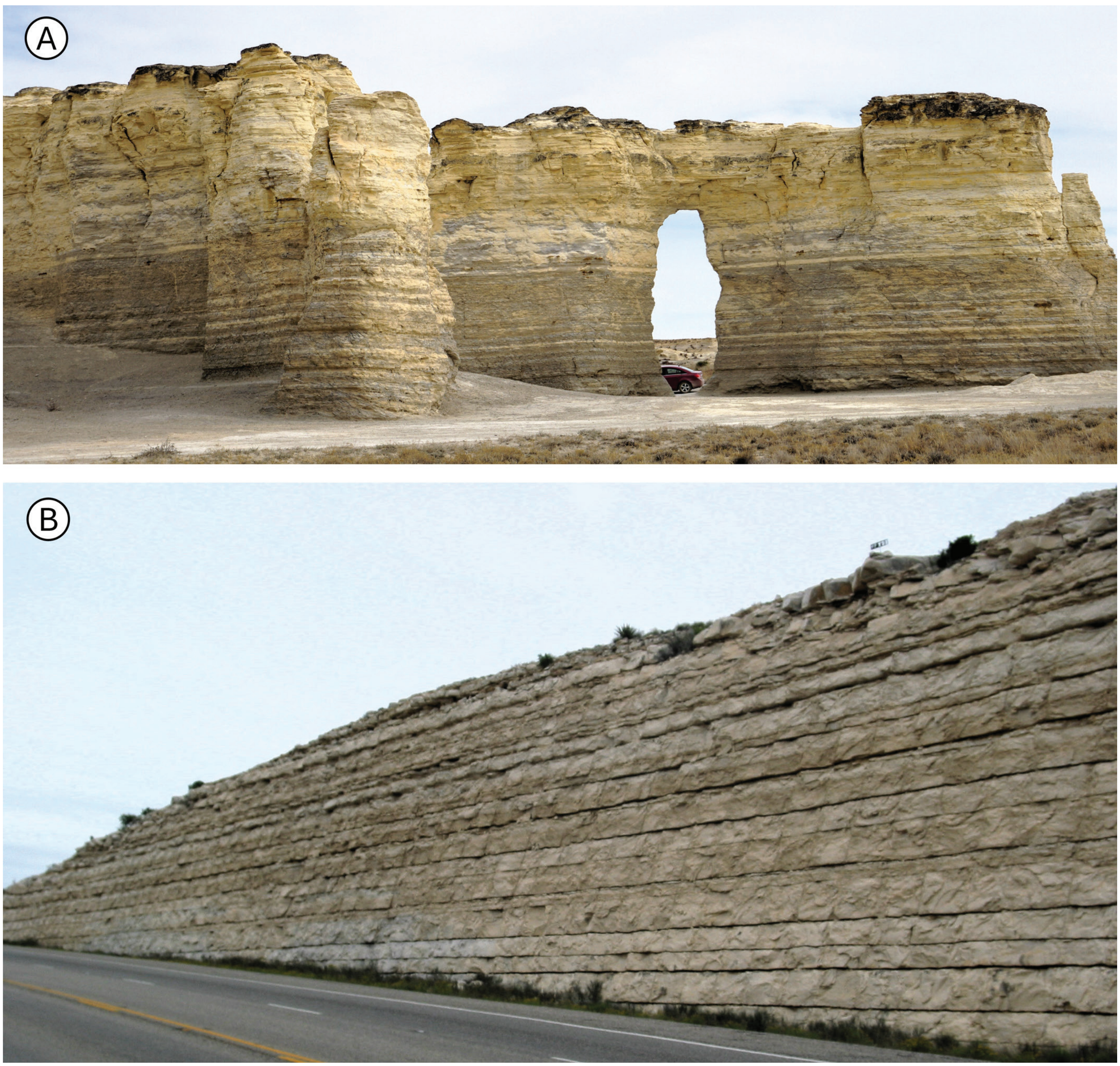

Figure 16. A: Outcrop of the Smoky Hill Member of the Niobrara Chalk at Monument Rocks, west-central Kansas. B: Outcrop of the Austin Chalk west of Langtry, TX. Outcrop locations provided in Table 1.

Waage, K.M., 1975, Deciphering the basic sedimentary structure of the Cretaceous System in the Western Interior, *in* Caldwell, W.G.E., ed., The Cretaceous System in the Western Interior of North America: Geological Association of Canada Special Paper, 13, p. 5581.

Yonkee, W.A., and Weil, A.B., 2015, Tectonic evolution of the Sevier and Laramide belts within the North American Cordillera orogenic system: Earth-Science Reviews, v. 150, p. 531593. https://doi.org/10.1016/j.earscirev.2015.08.001\

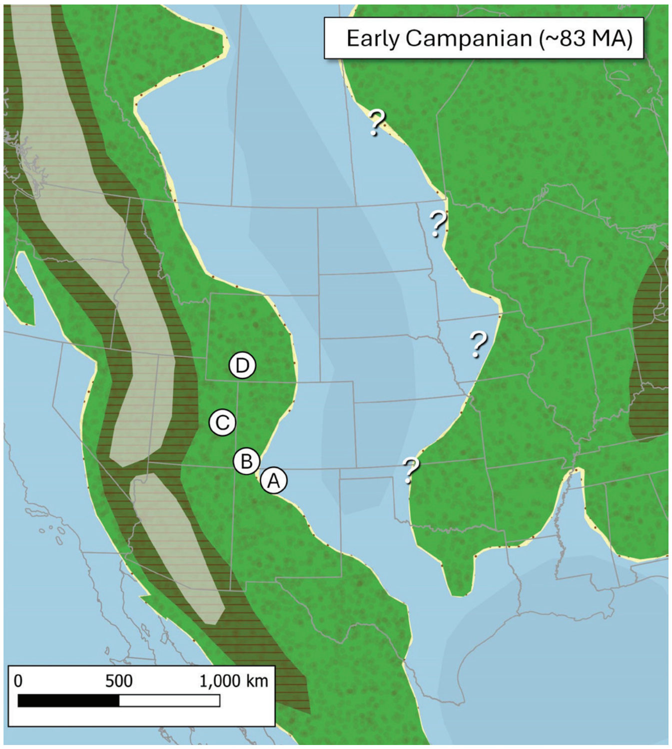

Figure 17. Schematic representation of early Campanian Western Interior Seaway paleogeography, redrawn and simplified from Blakey (2014). Green areas are land. The location of the eastern shoreline is speculative as it is not preserved. Lettered circles show locations of outcrops shown in Figure 19.

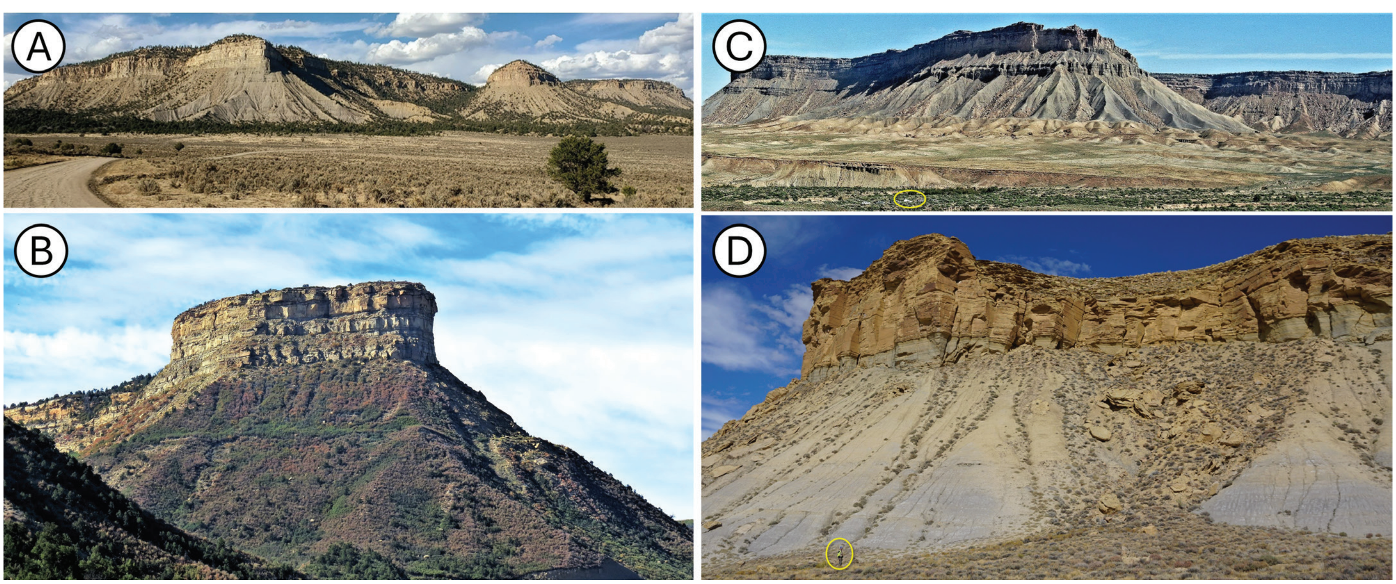

Figure 18. Lower Campanian shoreline deposits from various parts of the Western Interior Seaway. A: Point Lookout Sandstone west of El Vado Reservoir, north-central New Mexico. B: Point Lookout Sandstone at Point Lookout, southwest Colorado. C: Desert Member of the Blackhawk Formation, Hatch Mesa, central Utah. D: Brooks Member of the Rock Springs Formation, central Wyoming. Person circled for scale. Outcrop locations shown in Figure 17. Outcrop locations provided in Table 1.

Figure 19. Outcrop of upper Campanian deposits at Coal Canyon in western Colorado. Thick shoreface sandstones of the Rollins Sandstone Member of the Iles Formation are overlain by coal-rich nonmarine deposits of the Cameo-Wheeler coal zone of the Williams Fork Formation. This succession is time- and facies-equivalent to the Pictured Cliffs Sandstone and overlying Fruitland Formation in the San Juan Basin. Outcrop location provided in Table 1.